2. Hydrogen gas sensor utilizing a high proton affinity of pyrrolopyrrole derivatives

Introduction

1,4-Diketo-3,6-diphenyl-pyrrolo-[3,4-c]-pyrrole (DPP: Fig. 1(a)) and its derivatives are industrially important red pigments used as colorants in painting industries as well as in imaging areas.[2] Among these, a derivative with pyridyl rings (DPPP: diketodipyridylpyrrolopyrrole; Fig. 1(b)) is known to exhibit a high tinctorial strength of the red color in powders and possesses a high weatherfastness. However, the color suddenly changes from vivid red to dull red when a pigment-dispersed layer in polymers was prepared at elevated temperatures. Our in-depth study clarified that traces of protons are liberated from the polymer matrix at high temperatures and then protonates DPPP at the N atom of the pyridyl ring.[3] Our model experiment based on the vapor of nitric acid shows the spectral change as shown in Fig. 2(a).[3] To our great surprise, the electrical resistivity decreases remarkably due to protonation by five orders of magnitude (Fig. 2(b)), also accompanied by the appearance of photoconduction. On the basis of the present outstanding effect, we firmly believed that we can develop a sensitive, H_2-sensor by making use of a high proton affinity of DPPP. Then, our attention was focused on how to dissociate H_2 into protons. We have solved this problem by incorporating Pd or Pt layers into the sensor element. The H_2 sensor which we have successfully developed operates at room temperature in the following sequence: the first step is the dissociation of H_2 by means of a sputtered Pd-layer. The second sequence involves proton capture by the N atom of the pyridyl ring (proton acceptor) that releases an electron, leading to the changes in electrical conductivity.

This chapter deals with the sensing performance of 4'-pyridyl derivative (*para*-DPPP: Fig. 1(b)) upon exposure to H_2 together with those of 2'-pyridyl derivative (*ortho*-DPPP) and 3'-pyridyl derivative (*meta*-DPPP).

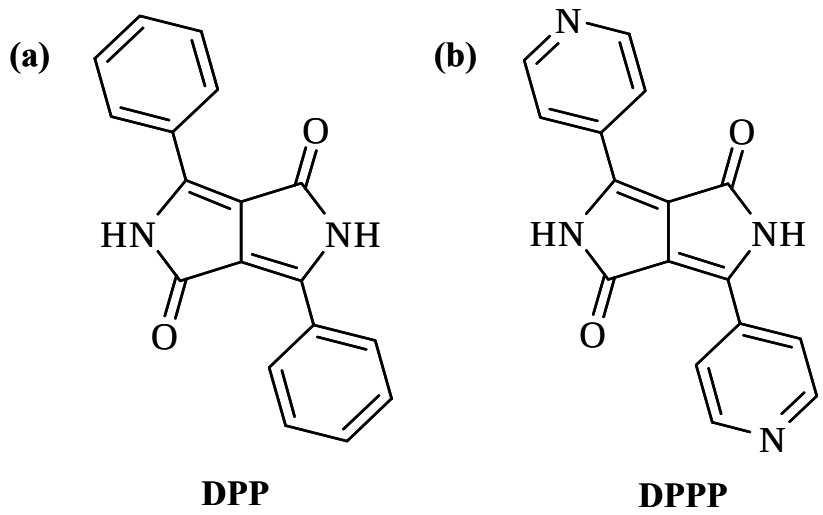

Fig. 1 Molecular conformation: (a) DPP and (b) DPPP.

Device structure

Al and ITO work equally good as the electrode. Furthermore, no significant difference is recognized in dissociation ability of H_2 between Pd, Pt, and Pd/Pt. Therefore, in the present report, the result is given for the device which includes ITO electrode used in combination with sputtered Pd. The device structure is ITO/sputtered-Pd/DPPP/ITO on the basis of the interdigital electrodes (Fig. 3). However, there are two ways to prepare a Pd-layer. One is to sputter Pd onto the ITO electrode, followed by the deposition of DPPP and vice versa. The former structure exhibits a better performance.

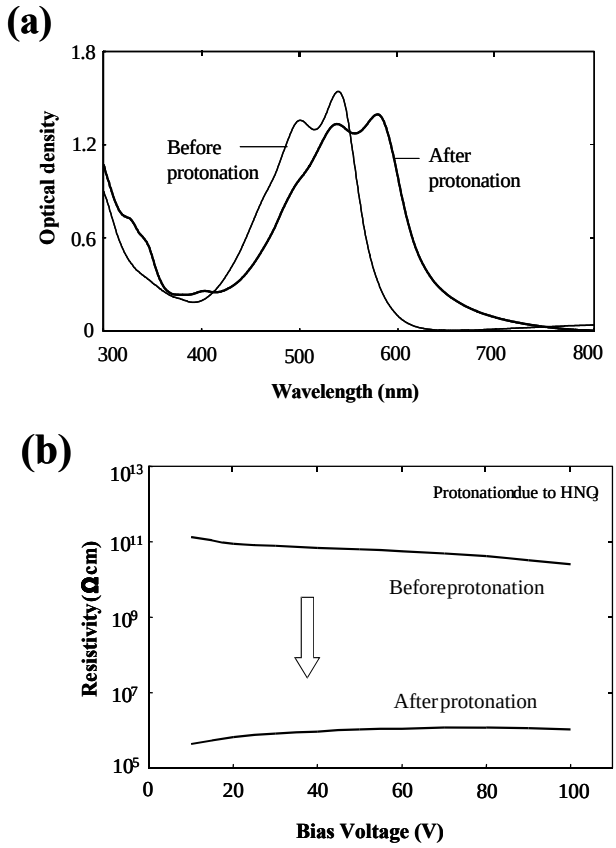

Fig. 2 (a) Absorption spectra of evaporated DPPP before and after protonation and (b) change in resistivity upon protonation.

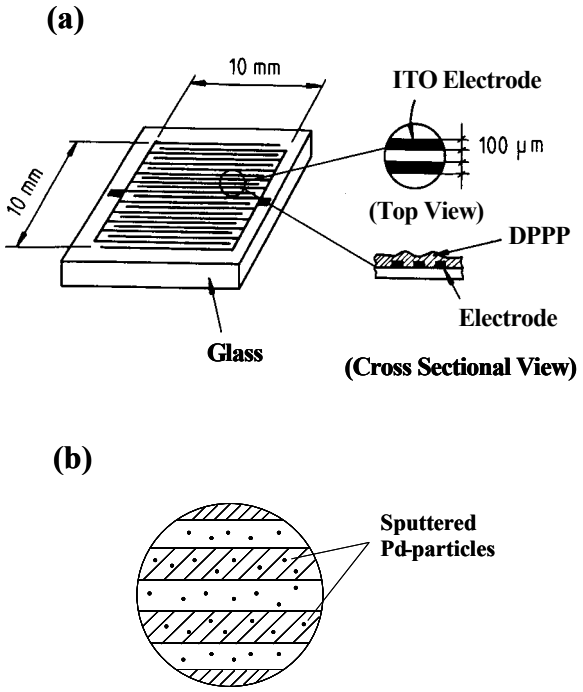

Fig. 3 (a) Interdigital electrodes and (b) magnified Pd-sputtered electrodes.

Synthesis and crystal phase used for the sensor

DPPP was synthesized according to the method described in Ref.4 and purified six times by sublimation, using a two-zone furnace.[5]

There are two crystal modifications in DPPP: phase I (grown from vapor phase)[6] and phase II (recrystallized from solution).[7] The projection of the crystal structure onto the molecular plane is shown in Fig. 4 for phases I and II. A striking difference is recognized between two modifications in the hydrogen bond network. Phase I is uniquely characterized by NH···O intermolecular hydrogen bonds between the NH group of one molecule and the O atom of the neighboring one. On the other hand, there exists another type of NH···N hydrogen bonds in phase II in addition to the NH···O bond. This NH···N bond is formed between the NH group of one molecule and the N atom of the pyridyl ring of the neighboring one. In phase I, two N atoms of the pyridyl ring remain free (*i.e.* unbonded) while one of the N atom is blocked by the NH···N hydrogen bond in phase II. Therefore, phase I is obviously more appropriate for H_2 sensors because two N atoms are available as the proton acceptor. Luckily enough, phase I is the phase as obtained by vacuum evaporation.

Fabrication of the sensor

The interdigital electrodes made of ITO were prepared by lithographic technique. Then, Pd was sputtered directly onto the electrodes by a sputter equipment (E-1030 Ion Sputter from Hitachi Corporation) in such a way as to form islands of Pd so as to avoid their contacts. After that, a thin layer of DPPP was applied by vacuum evaporation (Tokyo Vacuum Co. Ltd.: model EG240). The optimum thickness of Pd layer is about 3 Å while DPPP is deposited to the thickness of 300-400 Å.

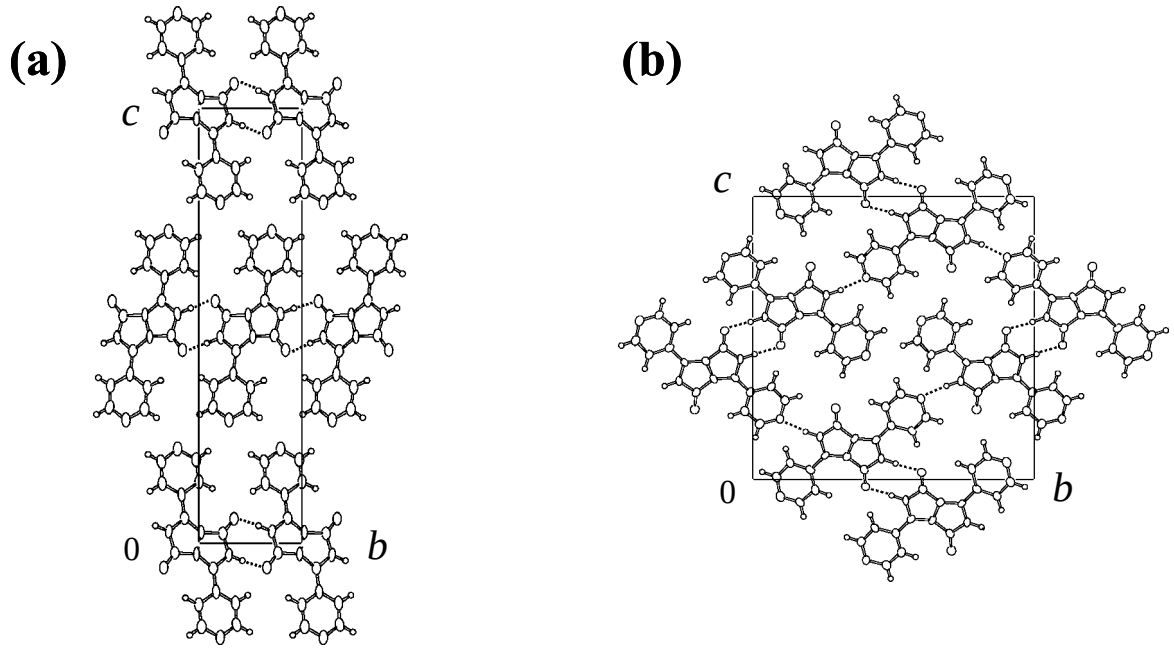

Fig. 4 Projection of the crystal structure onto the molecular plane: (a) phase I (*P*21/*n*, *Z* = 2, *a* = 3.722(1), *b* = 6.263(3), *c* = 26.506(9) Å, *β* = 94.41(2)°) and (b) phase II (*P21/c*, *Z* = 4, *a* = 3.695(1), *b* = 18.201(2), *c* = 18.456(2) Å, *β* = 4.68(1)°). There are four NH···O hydrogen bonds per molecule in phase I; whereas phase II comprises two NH···O and two NH···N hydrogen bonds per molecule.

Measurements of the sensor performance

Fig. 5 shows the experimental setup for measurements of the electrical resistivity. Upon exposure to H_2, the current induced was passed through a resistance of 100 kΩ connected in series with a bias voltage supply, and the voltage generated was then amplified by 10^3 times.

Influence of various gases on the sensor characteristics

The following gases were tested with a gas flow rate of 2 l/min.: CH_4 (1 %), CO (2 %), CO_2 (0.2 %), NO (0.6 %), SO_2 (23 %) and H_2O moisture.

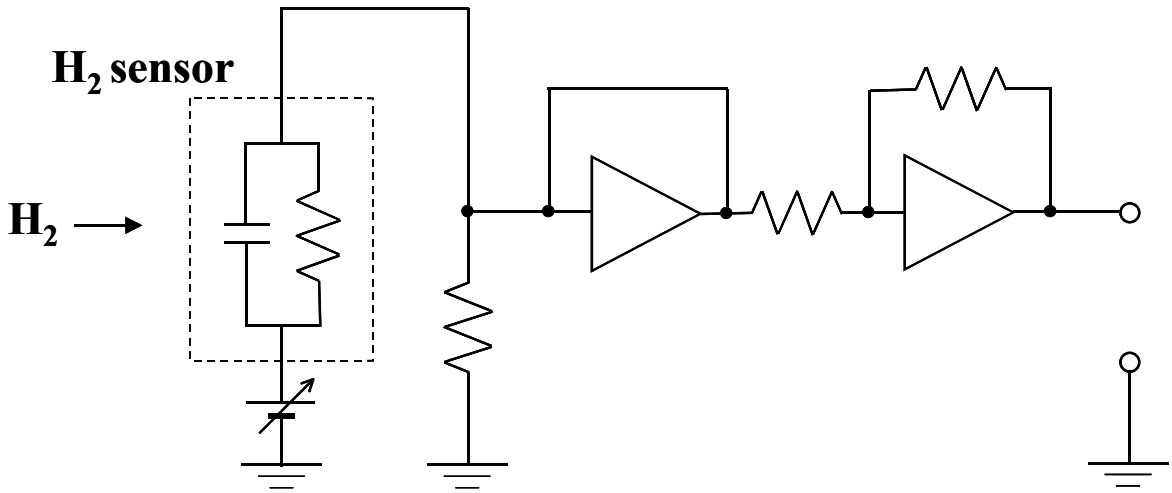

Fig. 5 Experimental setup for sensor measurements.

Results and Discussion

Performance of the H_2 gas sensor

Fig. 6 shows the change in resistivity of the sensor as a function of bias voltage when the sensor is exposed to 100% H_2. The resistivity decreases drastically by three orders of magnitude at room temperature. Although the initial resistivity is slightly higher at low bias voltage, no significant dependence of the bias voltage is observed. The resistivities for the H_2 concentrations of 0.05, 0.1, 1 and 10 % are shown in Fig. 7. It is remarkable to note that the resistivity diminishes by two orders of magnitude even for the H_2 concentration of 0.05 %. Furthermore, the resistivity is found to decrease linearly with increasing H_2 concentration, since Fig. 7 is a log-log plot of the resistivity and H_2 concentration. It is also to be noted that the initial resistivity shown in Fig. 6 is lower than that in Fig. 2(b). This is due to the sputtered Pd layer which makes the resistivity lower due to slight contacts between Pd particles. It is also important to mention that the sensor in the absence of the Pd layer exhibits no noticeable sensing effect.

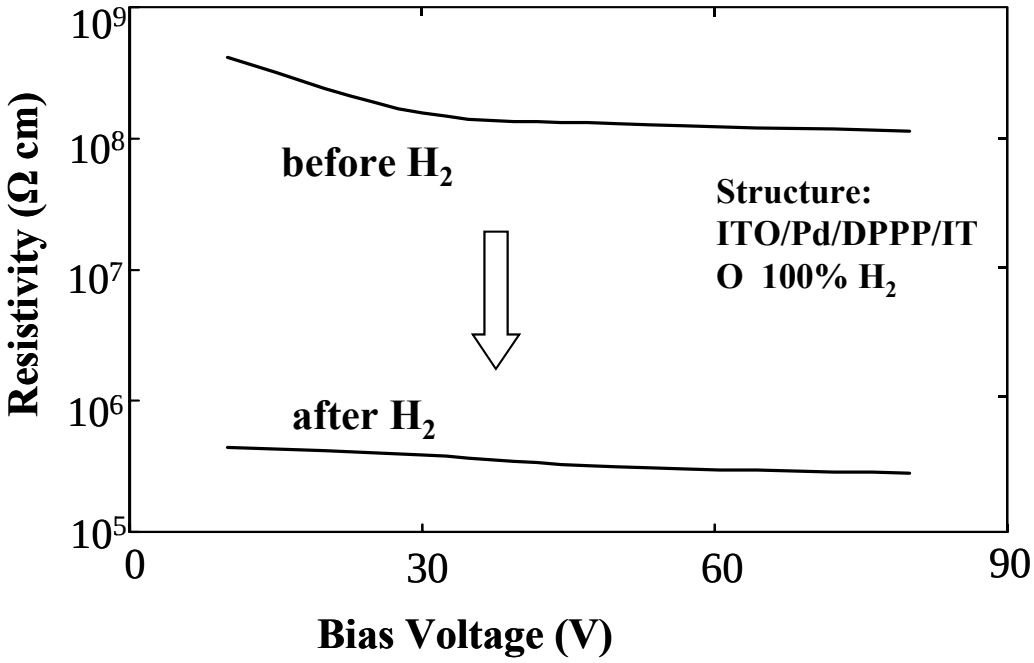

Fig. 6 Change in resistivity of the sensor before and after H_2 (100%) as a function of applied voltage. Cell structure: ITO/Pd/DPPP/ITO.

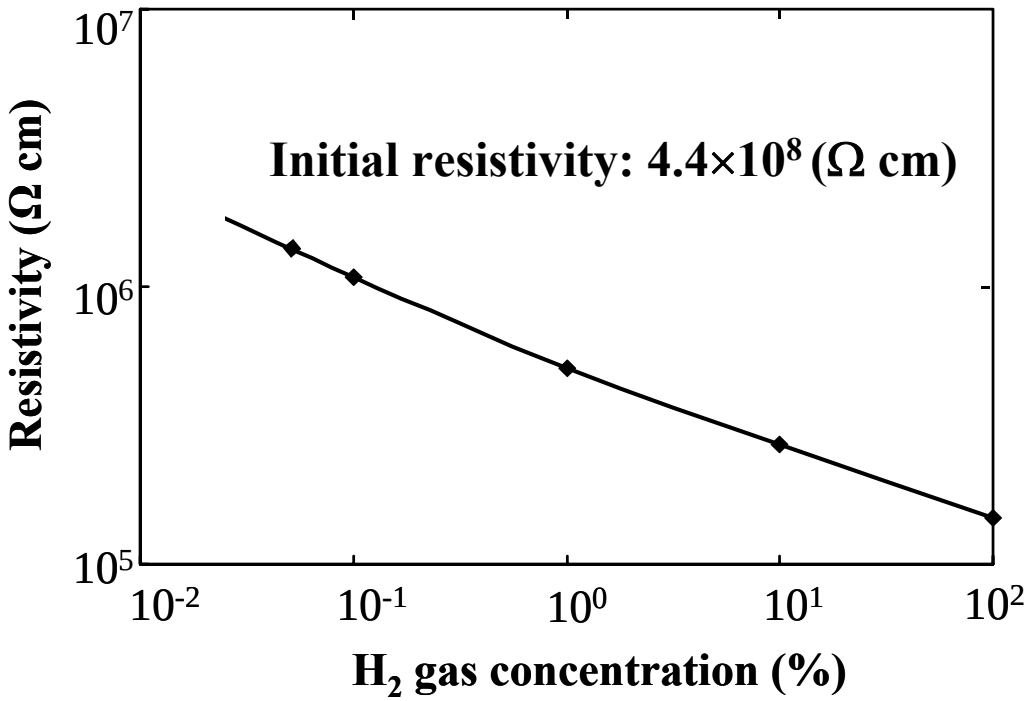

Fig. 7 Log-Log plot of the resistivity and H_2 concentration: 0.05, 0.1, 1, 10 and 100% H_2. Cell structure: ITO/Pd/DPPP/ITO. A resistivity change in two orders of magnitudes is achieved even for 0.05 % H_2.

Fig. 8 shows the build-up of the sensor signals as a function of time. The build-up time (80% of the maximum value) is about 400 m*s* where the gain is *ca* 900. This indicates that the response is quite rapid in the gain range of several factors. The signal builds up and builds down and then remains nearly constant. When H_2 is switched off, the signal decays and comes back to the initial state in five minutes. The return process is rather slow, but is still reversible. The reason why the signal builds down while the sensor is still exposed to H_2 is not yet fully clarified.

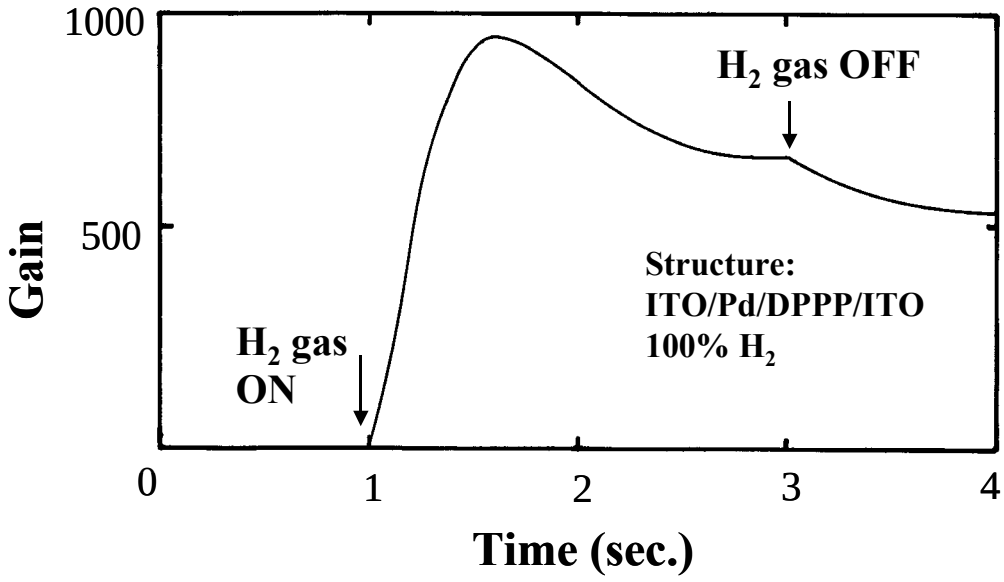

Fig. 8 Build-up of the sensor signal as a function of time. Cell structure: ITO/Pd/DPPP/ITO.

As for the influence of the various ambient gases on the sensor characteristics, no noticeable effect was observed (*i.e.* less than 0.1 % in resistivity).

In contrast to the outstanding effect of DPPP described above, the performance of *ortho* and *meta* DPPPs is quite poor as shown below. Fig. 9(a) shows the spectral change of *ortho*-DPPP before and after protonation due to the vapor of nitric acid. The H_2 sensor performance based on the structure of ITO/Pd/*ortho*-DPPP/ITO is given in

Fig. 9(b). The effect is quite insignificant. Similarly, the results for the spectral change as well as the sensor performance is given in Figs. 10(a) and 10(b), respectively. Here again, no noticeable effect is recognized. The common effect in *ortho* and *meta* DPPPs is characterized by rather low resistivity as compared with that of *para*-DPPP and also by little change in resistivity upon exposure to H_2.

Mechanism of the reduction in resistivity due to protonation

We believe that the reduction in resistivity (*i.e.* increase in electrical conductivity) takes place in the following reaction sequence. H_2 is initially adsorbed on the surface of DPPP and diffuse into the bulk where H_2 encounters sputtered Pd. Then, H_2 becomes unstable on Pd and can be dissociated into hydrogen atoms: H_2 (ads) $\rightarrow$ H (ads) + H (ads). At this moment, the N atom of the pyridyl ring of DPPP (strong proton acceptor) captures the proton which releases an electron as shown in Fig. 11(a). Since a high electric field is applied between interdigital electrodes (over 10^5 V/cm), the protonation process is presumably assisted by the electric field. Then, the released electron hops from one molecule to another as shown in Fig. 11(b), ending up with the increase in electrical conductivity. On the basis of the above mechanism, the present H_2 sensor is assumed to work also as an acid sensor. In fact, it works with a high sensitivity.

The situation in *ortho* and *meta*-DPPPs is obviously more complicated. The biggest issue is why the *para*-site is more influential on the electrical conductivity than the *ortho* and *meta* sites. This effect seems to be correlated with the electronic structure of DPP (Fig. 1(a)).[8] The mechanism is, however, not yet fully understood at the moment. The mechanism presented below is a speculation, but it is of interest and great help for developing an understanding of the mechanism of the electrical conduction. We have previously investigated the effect of deprotonation at the NH group by an alkali and its

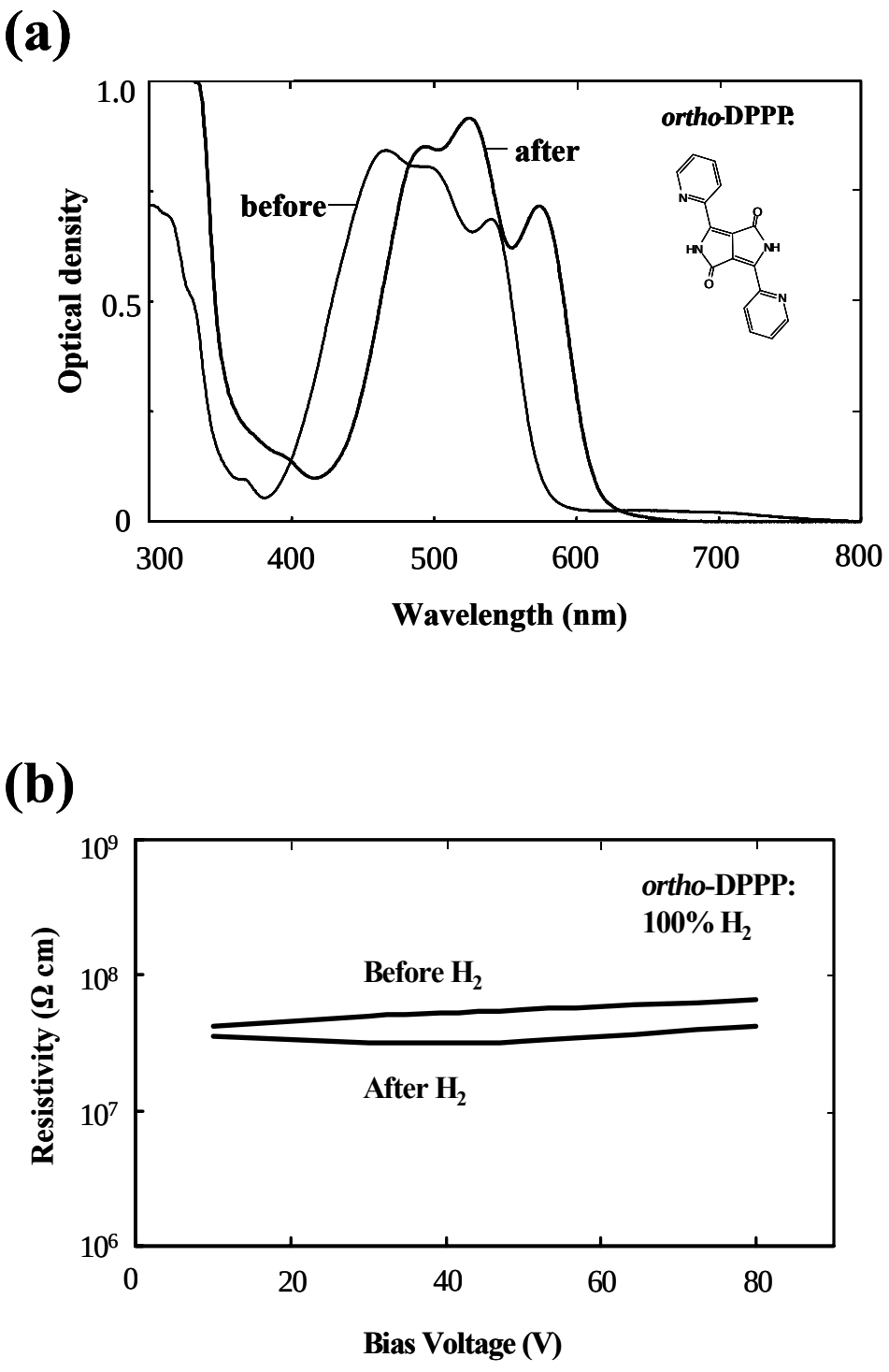

Fig. 9 (a) Absorption spectra of evaporated *ortho*-DPPP before and after protonation, and (b) change in resistivity of the *ortho*-DPPP sensor before and after H_2 (100%) as a function of applied voltage.
Cell structure: (ITO/Pd/*ortho*-DPPP/ITO).

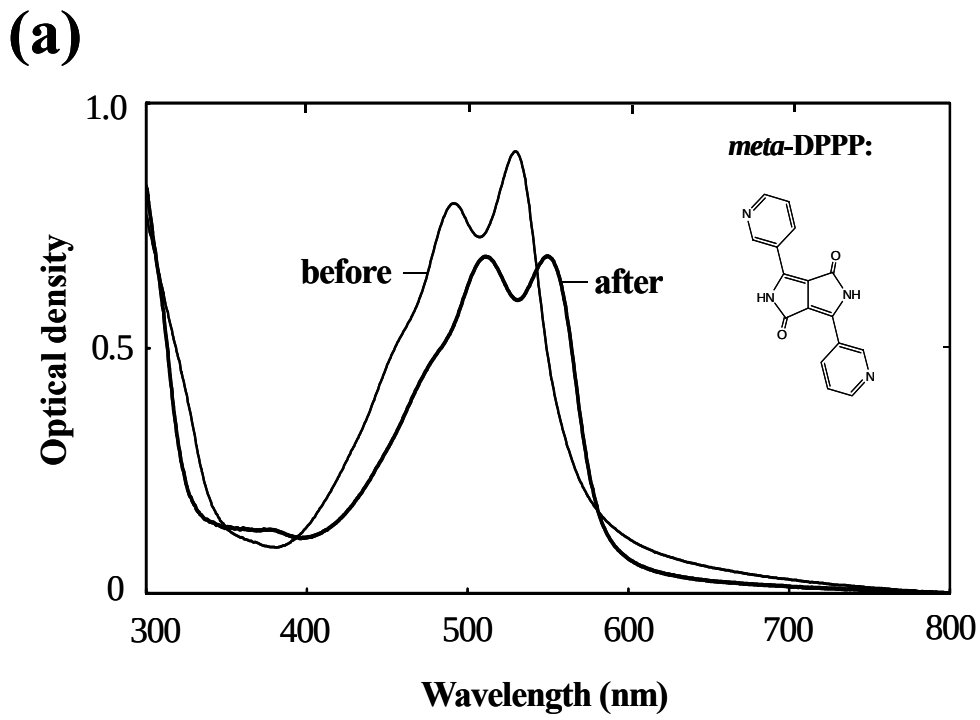

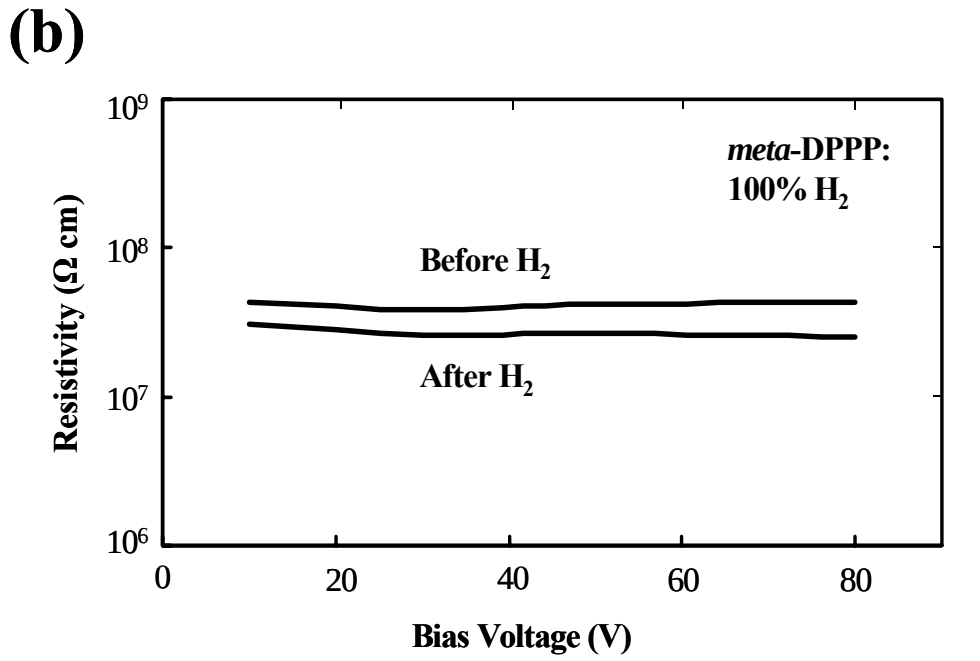

Fig.10 (a) Absorption spectra of *meta*-DPPP before and after protonation, and (b) Change in resistivity of the *meta*-DPPP sensor with Pd-layers before and after H_2 (100%) as a function of applied voltage.
Cell structure: (ITO/Pd/*meta*-DPPP/ITO).

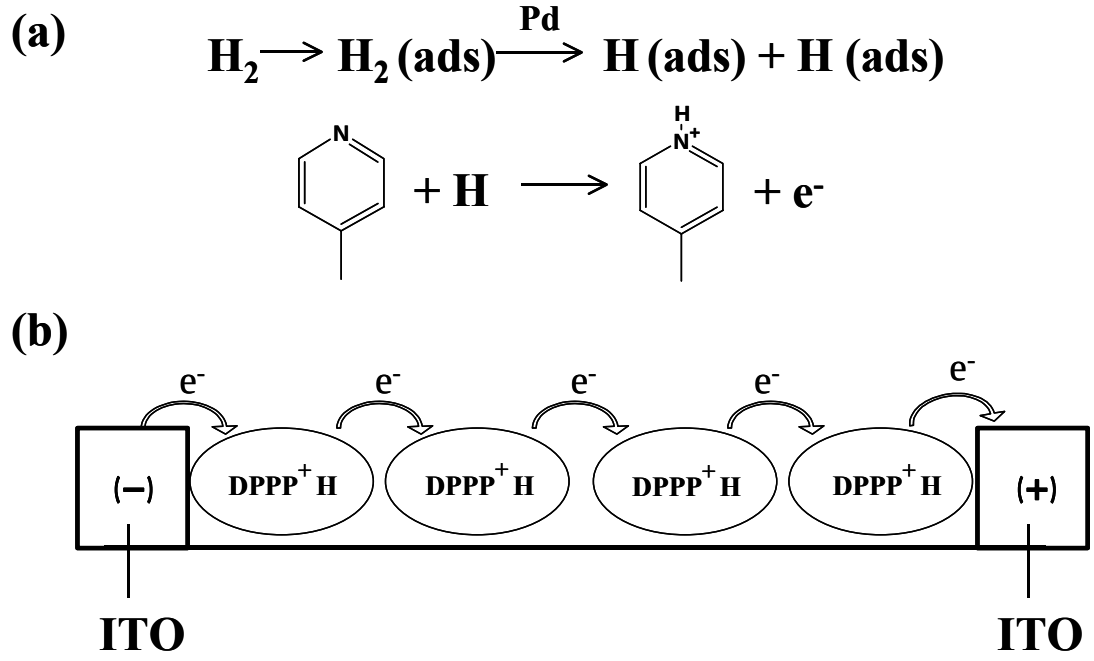

Fig.11 Proposed mechanism of the electrical conduction due to protonation: (a) dissociation of H_2 into H atoms and proton capture by the N atom of the pyridyl ring which releases an electron, and (b) hopping process of electrons from one molecule to another.

influence on the bathochromic shift by means of ^{13}C-NMR.[8] Deprotonation by NaOH in solution (*i.e.* >N^-) brings about a large bathochromic shift of 78 nm (*ca* 2650 cm^{-1}) on *mono*-deprotonation and 105 nm (*ca* 3400 cm^{-1}) on *di*-deprotonation. The present deprotontion is found to be well correlated with the electron delocalization as shown by ^{13}C-NMR. Table 1 summarizes ^{13}C chemical shifts of DPP, DPP/NaOH (1:1, *i.e.* *mono*-deprotonation) and DPP/NaOH (1:2, *i.e.* *di*-deprotonation) in dimethylsulfoxide-d_6. The chemical shift is more pronounced in *mono*-deprotonation than in *di*-deprotonation. It should be noted that the deprotonation at the NH group is well propagated throughout the chromophore. Especially, the influence on the *para*-site (No.7) of the phenyl ring is quite significant while rather insignificant on the *ortho* and

Table 1

^{13}C Chemical shifts of DPP, DPP/NaOH (1:1) and DPP/NaOH (1:2) in DMSO-d_6

C atom No*)	Chemical shifts (ppm relative to TMS)			
	DPP	DPP/NaOH (1:1)	DPP/NaOH (1:2)	Total change
1	144.0	155.3 (+11.3)	155.4 (+0.1)	+11.4
2	110.7	117.9 (+7.2)	118.7 (+0.8)	+8.0
3 (C = O)	162.4	172.0 (+9.6)	172.5 (+0.5)	+10.1
4	127.7	134.4 (+6.7)	135.6 (+1.2)	+7.9
5	128.9	128.0 (–0.9)	127.6 (–0.4)	–1.3
6	127.7	127.6 (–0.1)	127.5 (–0.1)	–0.2
7	131.7	128.5 (–3.2)	127.6 (–0.9)	–4.1

*) Partial chemical shifts are given in parentheses

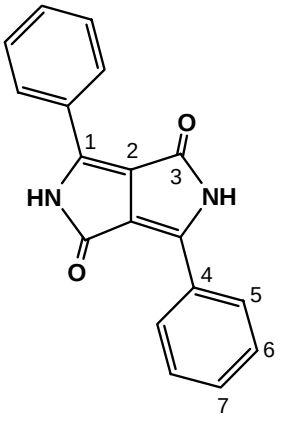

meta sites (No. 5 and 6, respectively). This indicates that the change at the *para*-site can be more effectively propagated throughout the chromophore. This means that the electron within *para*-DPPP is more mobile than that in *ortho* and *meta*-DPPPs. The present effect can closely be related to the difference in electrical conductivity between *ortho*, *meta* and *para*-DPPPs upon protonation.

Conclusions

A high-performance H_2 gas sensor has been developed on the basis of diketodipyridylpyrrolopyrrole derivatives. The sensing operation involves proton capture by DPPP which releases an electron, leading to the changes in the electrical resistivity. A reduction of resistivity by two orders of magnitude is achieved at room temperature for 0.05 % H_2. The process is reversible and the response time is about 400 m*s*. No noticeable effect of various ambient gases on the sensor was observed (*i.e.* less than 0.1 %). 4'-Pyridyl derivative (*para*-DPPP) is, by far, more sensitive than 2'-pyridyl (*ortho*) and 3'-pyridyl (*meta*)-ones.

References

1. M. L. Perry and T. F. Fuller, *J. Electrochem. Soc.*, **149**, S59 (2002).

2. M. Herbst and K. Hunger, *Industrial Organic Pigments*, pp.550-553, VCH, Weinheim, (1993).

3. J. Mizuguchi, *Ber. Bunsenges. Phys. Chem.*, **97**, 684 (1993).

4. A. C. Rochat, L. Cassar and A. Iqbal, *U.S. Pat.* 4, 579, 949 (1986).

5. J. Mizuguchi, *Krist. Tech.*, **16**, 695 (1981).

6. J. Mizuguchi, T. Imoda, H.Takahashi and H. Yamakami, *Dyes and Pigments*, **68**, 47–52(2005).

7. J. Mizuguchi, H. Takahashi and H. Yamakami, *Z. Kristallogr. NCS*, **217**, 519 (2002).

8. J. Mizuguchi and G. Wooden, *Ber. Bunsenges. Phys. Chem.*, **95**, 1264 (1991).